Supplementary information: A climate-conditioned catastrophe risk model for UK flooding

Paul D. Bates[1,2], James Savage[2], Oliver Wing[1,2], Niall Quinn[2], Christopher Sampson[2], Jeffrey Neal[1,2] and Andrew Smith[2]

[1]School of Geographical Sciences, University of Bristol, Bristol BS8 1SS, UK
[2]Fathom, Square Works, 17-18 Berkeley Square, Bristol, BS8 1HB, UK

Correspondence to: Paul Bates (paul.bates@bristol.ac.uk)

S1. Current UK flood hazard and risk datasets: further information

UK flood hazard and risk information at national and sub-national scales can be found in five broad classes of data product:

1. Floodplain zonation (i.e., hazard) maps for fluvial, coastal and sometimes pluvial flooding developed separately by government bodies in the devolved regions of the UK (Northern Ireland, Wales, Scotland and England) and predominantly used to inform land use planning decisions.

2. Flood risk maps or spatially aggregated risk data (i.e., the product of flood probability, exposure and vulnerability) also produced by the devolved administrations and predominantly used to inform flood defence investment policy and long-term risk planning.

3. Current and future flood risk estimates produced as part of the UK's Climate Change Risk Assessment process.

4. Flood hazard and risk data produced by commercial modelling firms at national scale, predominantly for use in the insurance and financial sectors.

5. Data on insured losses available from the Association of British Insurers.

These are described briefly in the main text, however further details for certain methods are provided below for interested readers.

S1.1 UK flood hazard maps in the devolved administrations

Government floodplain hazard maps show the land area likely to be inundated by specific low probability flood events and are compiled separately by the Department of Infrastructure Rivers in Northern Ireland (DfI Rivers), Natural Resources Wales (NRW), the Scottish Environmental Protection Agency (SEPA), and the Environment Agency (EA) in England. Each devolved region has its own mapping approach, and these differ in terms of the types of flood considered (pluvial, fluvial or coastal), the return periods that are modelled, whether or not flood defences are taken into account and how the maps are made

available to the public. Specifications exist for how this modelling should be conducted (see for example https://naturalresources.wales/flooding/developing-hydraulic-models-for-flood-risk   and
30 https://www.gov.uk/government/publications/river-modelling-technical-standards-and-assessment), but exactly what areas have been modelled using which methods is not recorded. To the authors' knowledge, the only recent attempt to collate metadata on the modelling undertaken in the four devolved regions of the UK into a single document was by Sayers (2017, see Appendix A, Table A1-1).

S1.2 UK flood risk maps in the devolved administrations

35 As well as the hazard maps discussed above, each devolved administration also produces an estimate of flood risk, either in terms of the number of properties exposed to flooding of a given probability, or the Average Annual Loss (AAL)/Expected Annual Damage (EAD). AAL and EAD are used interchangeably and represent the loss that would occur on average each year given a sufficiently long sample (AAL) or the loss caused by all possible flood events weighted by their probability of occurrence (EAD). For consistency we use the term Expected Annual Damage in this paper.

40 In England, flood risk maps are produced by the Environment Agency as part of their National Flood Risk Assessment (NaFRA) programme (Environment Agency, 2009). Data inputs to the system are updated several times a year as new information (e.g., new terrain data, new flood defences) become available, with major methodological updates every 5-10 years starting from 2004 and with the most recent being in 2018. NaFRA is an extension of the RASP methodology of Hall et al. (2003), which provided an early way of approximating national flood losses using a statistical-parametric approach.

45 RASP combined the Environment Agency's 1 in 1000 year return period hazard maps for fluvial and coastal flooding, a DEM, a vector layer identifying river centrelines and a national flood defence data base to make its calculations. Estimates of water depths within river channels for 40 different probability events from 1 in 1 year return period to 1 in 1000 are used to drive a flood defence reliability analysis to determine the volume of water entering the floodplain. We assume, as with the hazard maps discussed above, that these channel water levels are derived (either directly or indirectly) from analysis of historic river

50 flow data, however this is not clear in the RASP/NaFRA documentation (Environment Agency, 2009; Hall et al., 2003). In RASP and the original 2004 version of NaFRA, the water volume calculated by the reliability analysis is then spread over the floodplain DEM using simple non-hydraulic approximations to give the depth-probability exceedance curve in each 50m resolution model cell. Flood losses in NaFRA 2004 were then calculated using a national exposure database and the UK's standard set of depth damage curves (the so-called Multi-Coloured Manual approach, Penning-Rowsell et al., 2013). Spatial

55 correlations in flood depths (c.f. Heffernan & Tawn, 2004; Keef et al., 2009, 2012; Quinn et al., 2019) are not taken into account so only average annual losses can be computed and not the full loss-exceedance curve.

The methods underpinning the NaFRA analysis have changed significantly over time, but these modifications are rarely disclosed publicly. Indeed, it has taken significant detective work by Penning-Rowsell (2014) and Penning-Rowsell (2021) to uncover even limited aspects of the approach and differences from RASP. A major change occurred in 2008 when the simple

60 non-hydraulic method for floodplain depth estimation was upgraded to use HR Wallingford's Rapid Flood Spreading Model (RFSM). RFSM calculates inundation using a straightforward mass redistribution algorithm that does not conserve momentum. Whilst an obvious improvement on the parametric inundation calculations in RASP, RFSM has had only limited validation and has shown variable performance in the small number of tests that have been conducted (L'homme et al., 2009). Despite this apparent upgrade to the inundation calculation, raw output from NaFRA 2008 showed very high flood losses

65 (EAD of >£5Bn) as a result of excessive predicted floodplain water depths.

Penning-Rowsell (2021) has documented the significant and somewhat arbitrary adjustments that have been made to NaFRA since 2008 to try to combat this. Most significantly, the original depth-damage curve approach to computing losses was replaced with a simpler and cruder Weighted Average Annual Damages method (WAAD, following Penning-Rowsell & Chatterton, 1977) as this does not use the erroneous water levels. Instead, WAAD simply applies an average loss to each

70 property within the flood zone adjusted for different standards of protection and flood warning levels. Next, floodplain water depths are capped to be no more than the crest elevation of floodplain defences and computed losses for events below 1 in 30-year return period are set to zero. These changes do not have a physical basis but are instead required because simulation of small, non-valley filling floods can be difficult even with full hydrodynamic methods and the frequency of these events means that any mis-prediction can significantly bias the Expected Annual Damage. Finally, NaFRA data has been subject to

75 significant manual adjustment where the automated calculation yielded results that were considered implausible (Penning-Rowsell, 2021).

S1.3 The UK Climate Change Risk Assessment (CCRA) flood analysis

The Future Flood Explorer method discretizes the UK into Calculation Areas which represent either a few km of river channel or coast and its adjacent floodplain as delimited in national hazard and risk maps (the data described in the main text in Sections

80 2.1 and 2.2) or as 1km grid cells outside of this. The available UK hazard and risk data sets are interpolated to these zones and intersected with an exposure database detailing the locations and characteristics of all UK properties. For each Calculation Area an Impact Curve is then calculated which shows the number of properties flooded for each return period in the underlying sub-national data sets. Assumptions are made to extrapolate these Impact Curves to higher or lower return periods not represented in the underlying data, and Expected Annual Damage is calculated using the Weighted Average Annual Damage

85 method (Penning-Rowsell and Chatterton, 1977). Finally, standard regional climate change uplifts developed for the EA, SEPA, NRW and DfI (Kay et al., 2021) are applied to predict changes in future flood risk. This uses a simple method that relates the percentage change in flow, rainfall or coastal extreme water level to a change in return period. Finally, the flood damage due to this new return period is then interpolated from the existing Impact Curves. The third and latest CCRA report (denoted as CCRA3) was published in 2021 (Kovats and Brisley, 2021), but the Future Flood Explorer results it contains

90 (Sayers et al., 2020) used as input the risk modelling conducted by the devolved administrations in the UK that was undertaken around 2018.

S1.4 Comparing the outputs of current UK flood risk analyses

Table S1 summarises the results of the flood risk analyses described above. These values are the direct losses due to flooding only and have not been adjusted for inflation. The risk analyses from the UK's devolved governments and the Climate Change Risk Assessment (CCRA3) represent economic losses for both residential and non-residential properties, whilst the ABI data are residential financial losses only. In Section S2 we discuss the adjustments necessary to put these data on to a consistent basis, but here just the raw data are reported to ensure traceability back to the original sources. Examining Table S1 shows the extent to which the NaFRA analysis conducted by the Environment Agency has changed over time. Prior to January 2013 the analysis covered both England and Wales, but from that date onwards responsibility for flood risk management in Wales passed to a new separate body for that territory (Natural Resources Wales). Even allowing for this major change in territorial scope Expected Annual Damage has decreased markedly over time with the latest 2018 value (£0.66Bn) being nearly an order of magnitude less than the unadjusted 2008 value (£5.14Bn, see Table S1 note [f]). The number of properties exposed to flooding in England has stayed more constant over time suggesting that what is changing is not the area of flooding that is being predicted but the predicted water depth and how the loss calculation is being performed. Allowing for the differences in flood type and return period analysed, the proportion of properties exposed is similar in England, Wales and Scotland (somewhere around 1 in 6 or 1 in 7), whilst for Northern Ireland it is 1 in 19. Figures from the UK Climate Change Risk Assessment are, unsurprisingly, in line with the estimates from the devolved administrations given that it uses their data as a key input. What is more noticeable is the large differences between the modelled losses computed by the devolved administrations and the much smaller observed losses recorded by the Association of British Insurers (see Penning-Rowsell, 2021).

Source	Reference	Territory	Time period	Flood drivers quantified	Probability used in exposure calculation	Properties exposed (Residential and non-residential)	Average annual economic loss[a] (£Bn, uninflated[b], residential and non-residential loss unless specified)
Environment Agency NaFRA 2006	Penning-Rowsell (2014)	England and Wales	Not specified, but likely historical average conditions over the instrumental record[c]	Fluvial and coastal	0.1% Annual Exceedance Probability (AEP)	2.14M	1.41
Environment Agency NaFRA 2008	Environment Agency (2009) Penning-Rowsell (2014)	England and Wales	As above	Fluvial and coastal	0.1% AEP	2.40M[d] (~1 in 9 residential properties[e])	1.28[f]
Environment Agency NaFRA 2017	Penning-Rowsell (2021)	England	As above	Fluvial and coastal	0.1% AEP	2.66M	0.90
Environment Agency NaFRA 2018	Penning-Rowsell (2021)	England	As above	Fluvial and coastal	0.1% AEP	2.59M	0.66

Analysis	Reference	Region	Time period	Flood types	AEP	Properties	Losses
SEPA National Flood Risk Assessment 2018[g]	See website at note g. No peer-reviewed publication available	Scotland	As above	Pluvial, fluvial and coastal	Not formally specified[h], but likely to be 0.5% AEP	284k (~1 in 11 homes and ~1 in 7 business)	Not reported
NRW Flood Risk Assessment Wales 2021[i]	See website at note i. No peer-reviewed publication available	Wales	As above	Fluvial and coastal	0.1% AEP	245k[j] (~1 in 6 properties[k])	Not reported
Northern Ireland Flood Risk Assessment 2018[l]	Formal report available, see[m], but no peer-reviewed publication	Northern Ireland	As above	Pluvial, fluvial and coastal	1% AEP for fluvial, 0.5% AEP for pluvial and coastal	45k (~1 in 19 properties)	0.055[n]
UK Climate Change Risk Assessment (CCRA) 2021	Sayers et al (2020) Kovats and Brisley (2021, Sections 5.4.1.1.2 - 5.4.1.1.5)	UK	As above	Pluvial, fluvial and coastal	1.33 % AEP	~787k[o]	1.07[p]
Association of British Insurers (ABI)	Penning-Rowsell (2021)[q]	UK	1998-2018	Pluvial, fluvial and coastal	Not applicable	Not applicable	0.19[r] (residential losses only)

Table S1: Published outputs from UK flood risk analyses. See notes below for further details.

a. Direct losses due to flooding only. Does not include indirect losses.
b. Values are those produced at the time of the analysis and have not been adjusted for inflation.
c. Both the RASP and NaFRA documentation (Hall et al, 2003; Environment Agency, 2009) are unclear on this point. It seems likely that their analysis of flood magnitudes and water levels is based either on classical frequency analysis of river gauge data, or on regionalised flood frequency analysis which indirectly uses the same information. NaFRA

120 therefore most likely represents average conditions over the instrumental record. In the UK the majority of river gauges were installed in the period 1960-1990 (see https://nrfa.ceh.ac.uk/uk-gauging-station-network). The network currently comprises about 1500 measurement sites, but it is not clear how many of these are used in NaFRA or what time period is selected. NaFRA results therefore probably most closely represent an average for the period from approximately 1960 to the date of the analysis.

125 d. Plus, a further 2.8M properties exposed to an unspecified probability of surface water flooding. Most plausibly, this unspecified probability is 1% AEP as this is the rarest event considered in surface water flood maps for England (see https://www.gov.uk/check-long-term-flood-risk). This takes the proportion of properties exposed to ~1 in 6 which is the value quoted in Environment Agency (2009).

e. England property count in 2008 taken from
130 https://www.ons.gov.uk/peoplepopulationandcommunity/housing/datasets/dwellingstockbytenureuk

f. Figure obtained after: (i) switching to a simpler Weighted Average Annual Damage loss calculation from the originally used depth-damage function; and (ii) substantial manual adjustment to raw NaFRA2008 results by Environment Agency local teams. The unadjusted NaFRA 2008 result was £5.14Bn (Penning-Rowsell, 2013).

g. https://www.sepa.org.uk/environment/water/flooding/developing-our-
135 knowledge/#National_Flood_Risk_Assessment

h. SEPA's National Flood Risk Assessment mapped areas at risk of flooding with Annual Exceedance Probabilities of 10%, 0.5% and 0.1%. It is however unclear which zone has been used to determine the number of properties at risk. Examination of the graphics available at the web site in note g suggests that 0.5% AEP has been used.

i. https://naturalresources.wales/flooding/check-your-flood-risk-on-a-map-flood-risk-assessment-wales-map

140 j. See https://statswales.gov.wales/Catalogue/Environment-and-Countryside/Flooding/environment-and-countryside-state-of-the-environment-our-local-environment-properties-at-risk-of-flooding. This website gives a total of 88,588 properties at risk of river flooding, 67,724 from coastal and 129,858 from surface water flooding giving a total of 286,170, but a proportion of these structures will be a risk from multiple sources. Kovats and Brisley (2021) therefore give a total of 245,000 properties at risk from all flooding sources in Wales to account for this, although the NRW
145 reference that is given in support does not appear in Kovats and Brisley's bibliography. Nevertheless, this level of overlap between fluvial, coastal and surface water flooding seems plausible and the Kovats and Brisley (2021) figure is therefore used here.

k. Wales property count in 2019 taken from https://gov.wales/sites/default/files/statistics-and-research/2019-09/dwelling-stock-estimates-april-2017-march-2019-225.pdf

150 l. https://www.infrastructure-ni.gov.uk/publications/northern-ireland-flood-risk-assessment-nifra-2018

m. https://www.infrastructure-ni.gov.uk/sites/default/files/publications/infrastructure/northern-ireland-flood-risk-assessment-report-2018-updated-may2019.pdf

n. Interestingly, 74% of the EAD in Northern Ireland came from pluvial flooding in this analysis which is high compared to other devolved regions.

155 o. Kovats and Brisley (2021, Table 5.11) give the number of people exposed to a 1.3% AEP fluvial, coastal or pluvial flood event in the UK as 1.889M. Assuming an average UK household size of 2.4 (https://www.ons.gov.uk/peoplepopulationandcommunity/birthsdeathsandmarriages/families/bulletins/familiesandhouseholds/2020) gives the number reported here. In fact, this is simply reversing the calculation embedded within the Climate Change Risk Assessment analysis, which calculates properties flooded and multiplies this by occupancy
160 rates to get the people affected.

p. The Future Flood Explorer used in the Climate Change Risk Assessment calculates direct damage and increases this by 70% to account for indirect losses and a further 20% of the direct total to account for intangibles (Sayers et al., 2020, Table 4.1). Sayers et al (2020) report an EAD for direct losses, indirect losses and intangibles of £2.042M (Table 7.1), which implies the £1.07Bn figure for direct losses given here.

165 q. Mean of Table 4, column A in Penning-Rowsell (2020).

r. Penning-Rowsell (2021) note that the ABI data have a very different basis to the outputs from the sub-national scale flood risk analyses. ABI data are financial, not economic, losses and insurance market penetration by ABI members is <100%. See main text for details. It is the raw unadjusted ABI figures that are given here.

170 **S2. Like-for-like comparison of previous UK flood risk assessments**

Section S1.3 makes clear that current analyses report flood EAD in very different ways and consequently a number of adjustments to each measure are necessary to achieve a like-for-like comparison. For consistency we base the majority of our adjustments on the set of scaling factors determined in Penning-Rowsell (2021) as detailed below. For our work we report EAD data as financial losses in 2020 GB pounds (£) for England, Scotland and Wales only (i.e., Great Britain) as the necessary
175 data to undertake risk modelling for Northern Ireland are not yet available publicly.

For all existing UK risk analyses the following adjustments are necessary:

1. Adjust for inflation to 2020 values using data from the UK Office for National Statistics (ONS).

2. Convert territorial basis to Great Britain only. As Scotland and Wales do not report EAD values and because the value for Northern Ireland is only based on a simple GIS overlay, we scale the latest (2018) NaFRA value for England
180 to the whole of GB using the ratios reported in Penning-Rowsell (2021). These were taken from the emulation methodology used in the 2017 UK Climate Change Risk Assessment (Sayers, 2017). This suggested that England accounts for 79% of flood losses, Scotland 12%, Wales 6% and Northern Ireland 2%. To convert NaFRA values to a GB figure we therefore multiply by 98/79. To convert whole UK values from the CCRA and ABI to a GB value we multiply by 98/100.

185 For the upscaled NaFRA and CCRA3 values we also need to convert from economic to financial losses and therefore make two further adjustments for both:

    3. Add an allowance for betterment. This is the difference between the depreciated present-day value of a flood damaged item or property and the actual amount paid out or spent to replace it. Penning-Rowsell (2021) suggests that economic losses are only 62.5% of financial losses so we use this value to uprate the NaFRA and CCRA3 EAD values.

190   4. Add taxation. Economic losses do not include this element but to get to the actual sum lost UK sales tax needs to be added back in.

For NaFRA one final adjustment is necessary:

    5. Add an allowance for pluvial flooding. NaFRA values for EAD represent only fluvial and coastal flooding, whilst data from the CCRA, the ABI and our modelling additionally include pluvial losses. In both our modelling and the

195   modelling undertaken for CCRA3, the proportion of national flood losses that can be attributed to surface water is ~20%. We therefore uprate the NaFRA value by 25% to account for this.

The ABI data is already given in terms of financial loss but, following Penning-Rowsell (2021), four further adjustments are necessary for it properly represent the total national insured loss:

    6. Adjust for underinsurance. The ABI data only report financial losses for those people making an insurance claim, so

200   those without insurance or those who have insurance but choose not to claim are not included. Data on the scale of this issue is limited but what we do know comes from living cost survey data collected by the UK Office for National Statistics. This evidence is reviewed by Penning-Rowsell (2021) and we therefore use his conversion factor of 1.17 for this effect.

    7. Adjust for market share. Members of the Association of British Insurers represent only about 80% of the insurance

205   market so to convert to total insured losses for Great Britain an allowance must be made. For this we use the factor of 1.25 for this as determined by Penning-Rowsell (2021) following discussion with the ABI.

    8. Adjust for non-residential losses. As the ABI data represent losses to residential properties only, we need to add in an estimate for non-residential losses to give a total insured loss value. For this we use a factor of 1.79 from Penning-Rowsell (2021) based on data from floods in 2007, 2013/14 and 2015/16.

210   9. Normalize for changing Gross Domestic Product (GDP) to 2020 values. Unlike Penning-Rowsell (2021) we adjust the ABI data for both inflation and GDP. This is because over time not only do prices increase (inflation) but so too does the total asset stock (reflected in GDP). Flood losses in 1998 at the start of the ABI data reflect losses to the asset stock in place at that time. If the 1998 flood events were to happen in 2020 losses would be higher because of the development that has occurred between those dates.

215 Using these sets of adjustments, we can now put the NaFRA, CCRA and ABI values onto a similar basis. These data are given in table S2 below.

Source	NaFRA	CCRA3	ABI
Unadjusted EAD value (Billions, from Table S1)	£0.664	£1.07	£0.19
Adjusted EAD value (Billions)	£2.246	£2.154	£0.714

Table S2; Estimated Annual Damage given by existing flood risk model analyses (NaFRA, CCRA) and observations (ABI). Data are given as direct financial losses due to fluvial, pluvial and coastal flooding in 2020 values for residential and non-residential properties in Great Britain.

After adjustment, the NaFRA and CCRA3 values are extremely close, as one would expect given that both are based on the same data. The difference between both model analyses and the observed flood loss data from the Association of British Insurers is however stark, with observations being over three times smaller as previously noted by Penning-Rowsell (2021). We return to this comparison in Sections 4 and 5 of the main text.

S3. Methods

3.1 UK flood hazard layers

The flood hazard layers are the underlying dataset from which the stochastic model samples. The method used derives from the global inundation mapping approach of Sampson et al. (2015), but with numerous improvements due to access to higher quality data within the UK. In particular, the availability of terrain, hydrography, stream gauge, rainfall, and defence data in the UK transpires to produce a flood model of significantly enhanced accuracy compared to the Sampson et al. (2015) global model. Similar modelling has also been completed for the continental US (Bates et al., 2021; Wing et al., 2017) and was shown to be able to recreate the inundation extent predicted by high-quality local models to within typical input data and model structural error (Critical Success Index values in the range 0.78–0.87 for the 1 in 100 year return period flood; Bates et al., 2021).

The approach consists of the following steps:

1. Creation of boundary condition information for historical average fluvial, pluvial and coastal floods for ten different return period events from 1 in 5 to 1 in 1000 year.
2. Updating these boundary conditions for current and future scenarios using a change factor approach
3. Assembling topography, hydrography, and flood protection data.
4. Simulating the resulting inundation using a state-of-the-art hydraulic model.

Each of these steps is described in detail below.

3.1.1 Boundary condition estimation for historic average conditions

The input to the fluvial hydraulic model is, naturally, discharge of a given exceedance probability on every river reach in the UK. The dense array of river gauges with long historical records contained within the National River Flow Archive (NRFA) is used to predict extreme flows on every river (even those without gauges) via Regionalised Flood Frequency Analysis. We broadly follow the standard methods outlined in the UK's Flood Estimation Handbook (FEH; Robson & Reed, 1999) for this procedure, although the key difference in our approach is the use of open-source data within the flood estimation calculation and its consistent application across the UK. The methodology involves the calculation of an index flood for every river – in this case, the median annual flow (QMED; equivalent to the 2-year flow) – and a pooled growth curve which stipulates how to translate the index flood to a flood of any given exceedance probability.

QMED is computed at each of the ~350 highest quality NRFA gauges by taking the median of annual maximum flows (where gauge records are long enough) or using a peaks-over-threshold approach (where records are <13 years). We use maps of the same catchment characteristics as in the FEH procedure (catchment area, average annual rainfall, flood attenuation due to reservoirs and lakes, base flow index, standard percentage runoff and urban extent) but instead derive these from public sources. The relationships derived between QMED and the catchment descriptors thus enables the computation of QMED at any river location in the UK. Our QMED model versus observed QMEDs at each gauge location is shown in Figure S1, for which we obtain an R^2 value of 0.89.
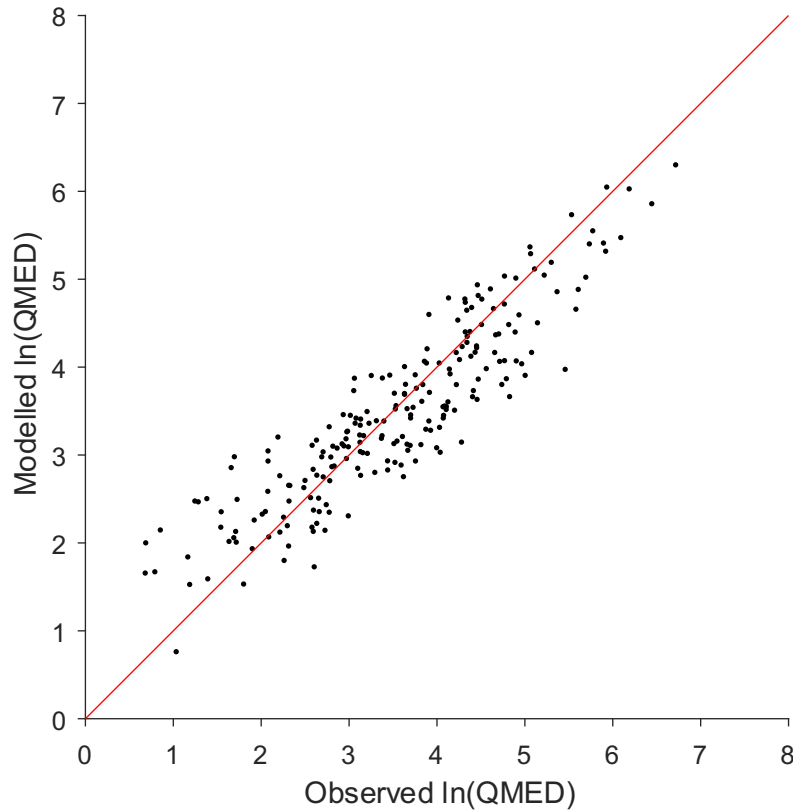
260 **Figure S1: Plot of observed vs. modelled index flood (natural logarithm of QMED in m^{3}s^{-1}).**

To translate QMED to any given extreme flow, a growth curve is required. Following the FEH approach, L-moments (Hosking, 1990) are computed for ~800 suitable gauging sites. These L-moments form the parameters of a Generalised Logistic distribution, describing the relative increase in magnitude of a given probability flood from its index. Since flood records are generally too short to understand extremes, this approach substitutes time for space by pooling together growth

265 curves from similar gauge locations. This produces an effective record of L-moments with lengths suitable for examining the tail. For a given ungauged location, gauges with similar characteristics are extracted and a pooled L-moment ratio is computed with preferential weights given to hydrologically similar sites and those with longer records. Flood frequency curves can then readily be computed at any location along the UK river network.

For the pluvial model, the required input is rainfall rather than river flow. Intensity-Duration-Frequency curves were calculated

270 from CEH-GEAR1h, an hourly gridded rainfall dataset at 1 km spatial resolution (Lewis et al., 2018). 1-hour, 6-hour, and 12-hour intensity-frequency relationships were computed.

Finally, boundary conditions for the coastal model consist of time varying water heights. Extreme water heights were obtained from the Environment Agency 'Coastal flood boundary conditions for the UK: update 2018' dataset (Environment Agency,

2019). This dataset provides estimates of extreme water heights in seas and estuaries around the UK at spatial intervals of approximately 2 km for multiple return periods. Each boundary condition location was mapped to its appropriate tide gauge as defined within the Environment Agency dataset and the relevant time varying storm surge profile (using the EA Design Surge Profile dataset) was applied to the surge element of the extreme water height. Normalised extreme coastal profiles were then calculated from UK tide gauge data using the 5 largest tidal events per year from up to 20 years of record at each gauge. These were then combined with the extreme water height estimates and design surge profile to produce time varying coastal boundary conditions for particular return period events around the UK coast.

3.1.2 Incorporation of climate scenarios

To account for flooding within a changing climate, a change factor approach was applied to the main components that drive the hydraulic model. This approach removes issues with model bias that would be present when taking absolute values from climate projections. In the case of the UK, 12km spatial resolution climate projections from the Met Office UKCP18 project for the RCP8.5 scenario were used, however loss results in this paper are presented in terms of specific global warming levels to decouple from the specific climate scenario that was simulated. To do this, we find the global mean temperature increase of each explicitly simulated scenario (2030, 2050 or 2070) and then calculate interpolants in cases where a warming level falls between simulations. These interpolants are then used to calculate the water depths relevant to each global warming level.

Changes in extreme precipitation between historical and present day, 2030, 2050 and 2070 under RCP8.5 were calculated by taking the median change in 1 in 2-year return period precipitation across the climate model ensembles at their native 12 km grid resolution. These change factors were then used to perturb the rainfall component in the pluvial model simulations. For the pluvial model, infiltration rates are calculated using a modified Horton equation based on soil type, and drainage standards are estimated for urban areas.

For the fluvial model, precipitation and temperature projections from the UKCP18 12km data were used to force the HBV-light rainfall-runoff model (Seibert and Vis, 2012) to obtain simulated streamflows at ~1000 locations across the UK. Streamflow at these locations was simulated 10 times, each time with a different set of calibration parameters in order to account for first-order uncertainty in parametrization of the rainfall-runoff model. Model performance was similar to that obtained using the HBV-light model applied in a similar manner to US catchments (Bates et al., 2021). Streamflow simulations were carried out for historical, present day, 2030, 2050 and 2070 climates using the same UKCP18 12km rainfall data employed for the precipitation change analysis. Later, changes in the 1 in 2-year return period river flow under present day and future (2030, 2050 and 2070) scenarios were applied to the historical fluvial inundation model boundary conditions (i.e., return period flow magnitudes from the RFFA) to obtain fluvial flooding under a changing climate.

For the coastal model, our future scenarios consider sea level rise resulting from future climate change using estimates made by Kopp et al. (2014). These are a set of estimates of sea level rise at tide gauge locations across the UK for various scenarios and time horizons (including RCP8.5). Times not explicitly included (such as 2070) are estimated by interpolating between

available time horizons (e.g., 2050 and 2100). The computed spatial distributions of change factors for river flow, rainfall and coastal extreme water level are shown in Figure S2. Importantly, these factors are materially different to current climate change allowances produced by Kay et al. (2021) for the devolved administrations in the UK. For example, for England these are uniformly positive for rainfall (+25 to +50% for all regions and time periods) and nearly always positive for river flow (-7% to +127%) (see https://www.gov.uk/guidance/flood-risk-assessments-climate-change-allowances). Negative changes in river flow only occur in four out of 92 catchment areas and only in 2050, all in the east of England, and in no catchments by 2080. In Wales (see https://gov.wales/climate-change-allowances-and-flood-consequence-assessments) changes in river flow by 2050 and 2080 range from +5% to +75%, whilst in Scotland (https://www.sepa.org.uk/media/594168/climate-change-guidance.pdf) the range for river flow by 2100 is +34% to +59%.
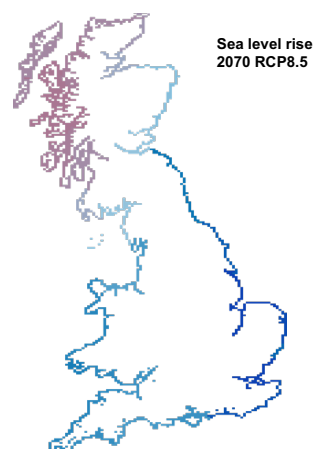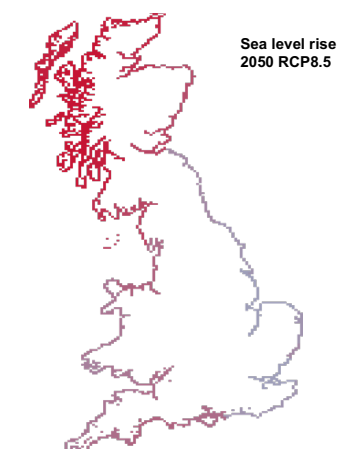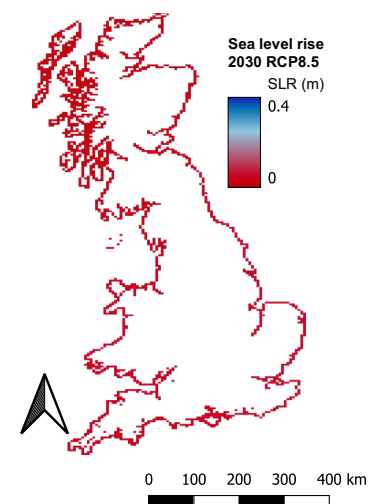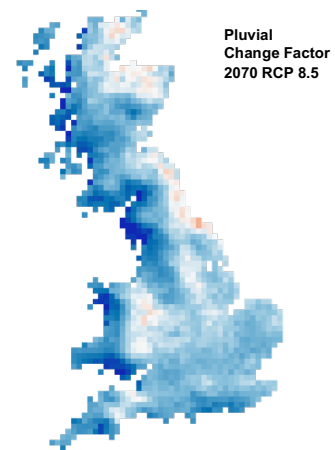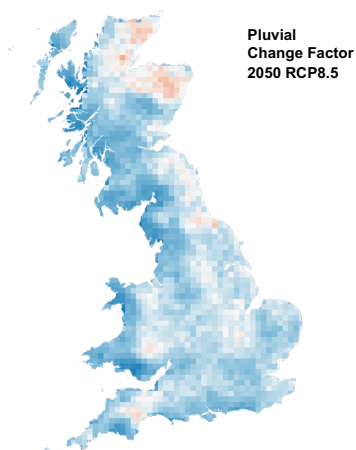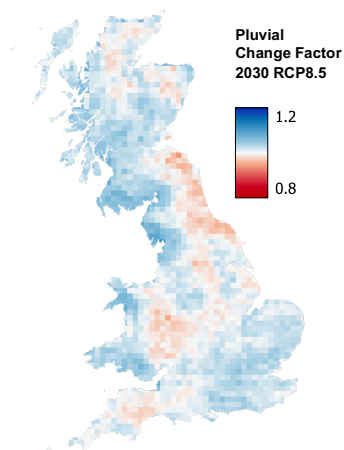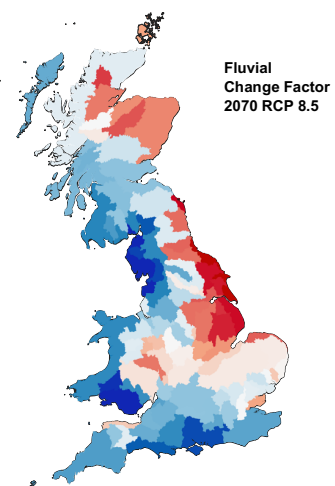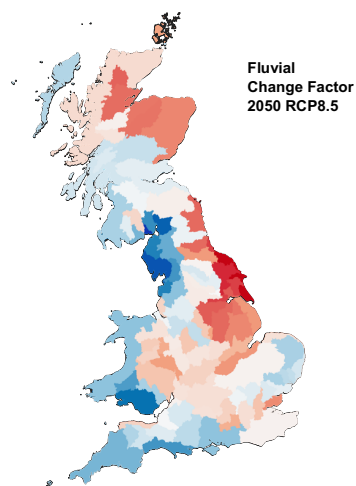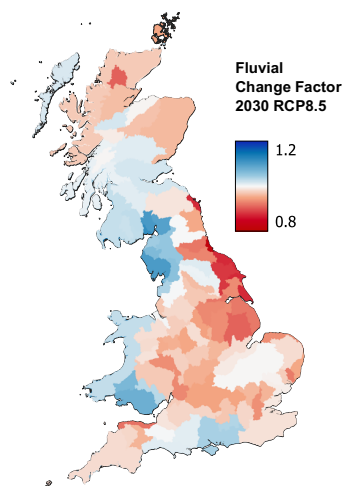
Figure S2: Fluvial, pluvial and coastal change factors by 2030, 2050 and 2070 used in the model. For rainfall and river flow changes are given as a multiplicative factor relative to the historic record (~1960-present, centred approximately on 1995), whilst for increases in sea level are given in metres from a 2018 baseline.

3.1.3 Topography, hydrography, and flood protection data

The hydraulic model is executed at 1 arc second resolution (~20-25 m at this latitude) across the UK using a composite Digital Elevation Model (DEM) built using the latest airborne LiDAR data from the relevant government agencies, alongside UK Ordnance Survey terrain data. Around 160,000 km^2 (or ~70%) of UK land area is covered by airborne LiDAR, which has a typical vertical RMSE against ground surveys of flat hard targets of <10cm. By design, and fortuitously for this study, LiDAR coverage is concentrated in the river and coastal floodplain areas with which we are here most concerned. In areas where LiDAR does not exist, we use the UK Ordnance Survey Terrain 50 DEM (https://www.ordnancesurvey.co.uk/business-government/products/terrain-50).

Channel locations are defined by combining the open-source UK Ordnance Survey Rivers dataset (https://www.ordnancesurvey.co.uk/business-government/products/open-map-rivers) with a DEM-based analysis using the TopoToolbox software (Schwanghart and Scherler, 2014) for headwaters areas. The drainage area at any point along the river network is required to predict extreme flows (see section 3.1.1), so a flow accumulation grid is constructed using the DEM and channel location data. While river bathymetry information is not available over wide areas, it must at least be approximated to enable behavioural simulations of flood events (Fewtrell et al., 2011). River widths are derived based on empirical relationships with upstream catchment accumulation area i.e., a hydraulic geometry approach. Channel bed elevations are then the last remaining variable to be estimated (as rectangular channels are assumed). By assuming a bankfull discharge return period of approximately 1 in 2 years (Andreadis et al., 2013; Harman et al., 2008; Leopold and Maddock, 1953), the flow generation procedure described in the preceding section is able to yield an estimate of channel conveyance capacity. By combining bankfull discharge, channel width, and bank heights calculated from the DEM, it is then possible to produce an estimate of channel depth using an optimization solver based on the gradually varied form of the 1D shallow water equations (Neal et al., 2021). Linking channel geometry to discharge return period in this manner ensures that the channels are appropriately sized for the flows being simulated, mitigating the problem of gross mismatches between discharge and channel conveyance.

A further consideration essential for accurate flood risk mapping is the influence of defences on conveyance capacity and inundation patterns. We explicitly incorporate data from various national government agencies (mostly the Environment Agency in England and Natural Resources Wales) to ensure structural protection measures are accounted for in the fluvial and coastal models. There are some locations, particularly in Scotland, where such information is missing, so we apply a levee detection algorithm to fill in these gaps (Wing et al., 2019). This algorithm searches for levee-like features in the high-resolution terrain, and ensures their elevation is maintained in the 1 arc second grid. This means other hydraulically important features that may not formally be flood control structures, but which have a flood controlling effect (for example causewayed roads), are also properly represented in the model.

3.1.4 Hydraulic modelling

Hydraulic modelling is conducted using an implementation of the LISFLOOD-FP hybrid 1D/2D numerical scheme (Almeida et al., 2012; Almeida and Bates, 2013; Bates et al., 2010). This solves the local inertial form of the shallow water equations in 2D over the floodplain using a highly efficient explicit finite difference scheme on a staggered grid which yields second-order accuracy in space on a compact, local stencil (Shaw et al., 2021). Combined with improvements in implementation and optimisation through parallelization on central and graphical processing units, this has provided dramatic reductions in model runtimes, vital for applications across national to continental scales (Neal et al., 2018; Neal et al., 2010).

An important limitation of many 2D approaches over large domains is the inability to represent rivers whose width is considerably smaller or larger than the grid size. Neal et al. (2012) addressed this issue within the LISFLOOD-FP model through the implementation of a 'subgrid' solver in which channel characteristics and flows are represented using a 1D local inertial model, while floodplain flows occurring when channel conveyance capacities are exceeded are propagated using the 2D inertial model solver described above. Neal et al. (2012) validated this model implementation over an 800 km reach of the River Niger in Mali by comparing four different model structures: 1D only (no floodplain), 2D only (no channels), coupled 1D/2D (main channels with floodplain), and a 2D subgrid model (main channels, smaller subgrid floodplain channels, and floodplain). The study determined that inclusion of both the channel network and floodplain was essential, and that inclusion of the smaller subgrid channels on the floodplain yielded significantly increased simulation accuracy in terms of water level, wave propagation speed, and inundation extent.

This 1D/2D hybrid model enables all river channels in the UK to be explicitly modelled. Rivers with upstream accumulations <50 km^2 are not represented in the fluvial model since their flows cannot be accurately predicted by the Regionalised Flood Frequency Analysis as they are largely ungauged. Flooding in these headwater catchments is instead represented by the pluvial model, since the flood behaviour of very small catchments is effectively pluvial in nature anyway. The pluvial model involves gridded rainfall intensities of given duration and probability being input directly onto the 2D grid, with, importantly, 1D subgrid channels retained. The coastal model also includes 1D subgrid channels in combination with water height boundaries along the coastline to allow coastal flood waters to propagate both inland and upstream.

3.2 Stochastic catalogue generation

The UK hazard layers detailed above provide national estimates of inundation extent and water depth for 10 different return period event magnitudes (5, 10, 20, 50, 75, 100, 200, 250, 500 and 1000 years) at 1 arc-second resolution (~20-25m at this latitude). On their own these layers would allow national scale Expected Annual Damage (EAD) to be computed. However, to understand more fully the risk to assets or interests over large regions (for instance, the insurance market or flood emergency responders) it is vital to understand the joint probability (or spatial dependence) of an event impacting many catchments at the same time (often termed the flood footprint). The stochastic modelling component aims to address this requirement by characterising the spatial dependence in flooding across data from the UK river gauge network, gridded CEH-GEAR rainfall

datasets and a UK tide-surge model. The spatial dependence in extreme flows is determined using a conditional exceedance statistical model (Heffernan & Tawn, 2004; Keef et al., 2009, 2012) and this information is then used to sample plausible events from the pre-computed hazard layers (c.f. Quinn et al., 2019). By computing financial losses for each event, we can obtain the full loss-exceedance probability distribution.

Daily river flow time series used to train the conditional exceedance model were obtained from the NRFA dataset. This data set contains approximately 1400 gauging station records of varying length and quality. In terms of rainfall, 6 hour maximum daily rainfall records were obtained for Great Britain from CEH-GEAR1h (Lewis et al., 2018), whilst for Northern Ireland daily rainfall totals from CEH-GEAR (Keller et al., 2015) were used instead as sub-daily data were unavailable for this territory. Rainfall data were sampled from each 1 km gridded dataset with a greater density of sample points near areas with a greater population density. To ensure consistency between both fluvial and pluvial datasets we select only sites with a 24-year record from 1990 to 2014 that contain fewer than 15% erroneous or missing data and which have no obvious step change or trend in extreme flows over the measurement period, as determined by a Kendall Tau rank correlation coefficient test. Time series data gaps within the set of retained sites were infilled using regression relationships with neighbouring gauge time series. Maximum daily water heights were extracted along the UK coastline from an ERA5 reanalysis simulated by the Deltares Global Tide and Surge Model (GTSM; Muis et al., 2016) version 3.0 that computes coastal water heights at a 10 minute interval. Outputs from the GTSM were used for the same 1990-2014 period and filtered to ensure that only the nearest model output location to the centroid of each coastal catchment were retained. The resulting dataset comprises 604, 668 and 248 high quality, long-term fluvial, pluvial and coastal timeseries, respectively (Figure S3).
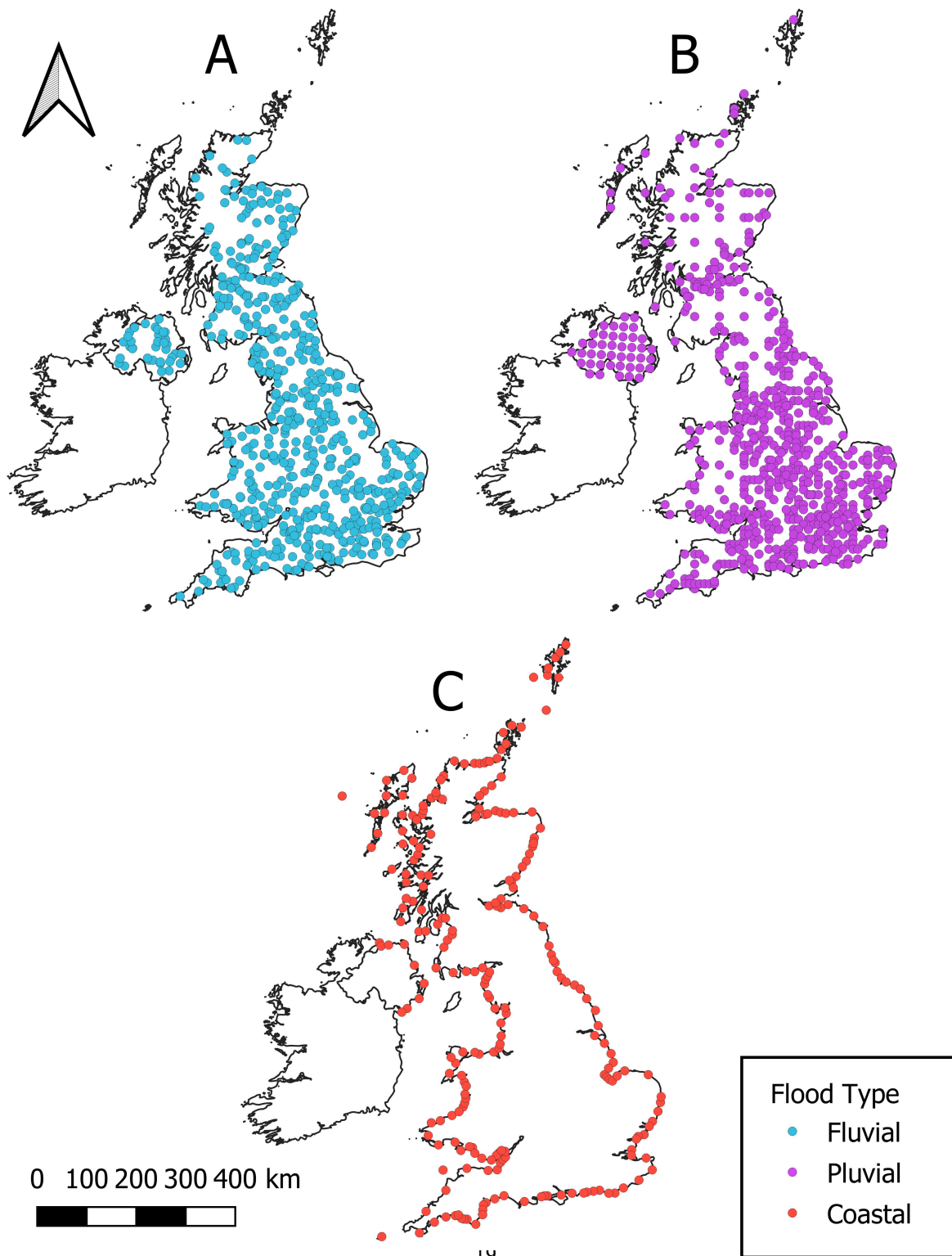
Figure S3: River flow gauges (blue), pluvial data points (purple) and coastal data points (red) used to define the spatial dependence.

405 The conditional exceedance model comprises two independent steps: first, the marginal probability distribution (defining the flow exceedance probability) is defined for each gauge site. Then, the dependence structures between sites are computed as a series of pairwise regressions. The marginal distributions were calculated using a semi-parametric function that fits a generalised Pareto distribution to time series values above a specified quantile threshold and an empirical distribution to those below it.

410 The tail dependence between a specified extreme gauge and its neighbours is then calculated as a series of pairwise regressions with associated residuals. Dependence between neighbours is modelled non-parametrically using the joint distribution of the residual terms:

$$\boldsymbol{Y}_{-i}|Y_i = \boldsymbol{a}Y_i + Y_i^{\boldsymbol{b}}\boldsymbol{Z}_{-i} \quad \text{for} \quad Y_i > v \tag{S1}$$

Where $\boldsymbol{Y}_{-i}$ is a vector of the marginal distributions at each gauge excluding gauge Y_i, v is a high threshold above which
415 dependence is modelled, $\boldsymbol{a}$ and $\boldsymbol{b}$ are vectors of parameters (limited to $-1 < \boldsymbol{a} < 1$ and $\boldsymbol{b} < 1$, respectively) describing the strength of the dependence and how it changes with increasing magnitude of Y_i, and $\boldsymbol{Z}_{-i}$ is a vector of residuals. Equation S1 is implemented in a pairwise manner so that the jth element of $\boldsymbol{Y}_{-i}$ is modelled as a function of Y_i using parameters $a_{j|i}$, $b_{j|i}$ and residuals $Z_{j|i}$, while the dependence between components of $\boldsymbol{Y}_{-i}$ are modelled non parametrically using the joint distribution of the residual $Z_{j|i}$.

420 To account for temporal lags in the flood peaks between sites, the dependence is calculated against all lags within a specified time window (after Keef et al 2009). Therefore, the conditional model becomes:

$$Y_{j,t+\tau}|Y_{i,t} \tag{S2}$$

where τ is a selection of temporal lags.

To reduce spurious correlation, temporal limits need to be set. A temporal window of 6 days is implemented to account for
425 the variability in arrival time of a flood peak between sites experiencing the same event. This window was selected given the relatively short lengths of rivers in the UK, and because Allen et al. (2018) show that, globally, flood waves take a median travel time of 6, 3 and 2 days to reach their basin terminus, the next downstream city, or the next downstream dam, respectively. Thus, the time taken for a flood wave to pass through downstream gauges in the UK is likely to be < 6 days. We do not impose any spatial limitations in the UK. An 'event' in this application, therefore, can be defined as a spatial footprint delineating the
430 gauges that may be in flood (hazard intensity greater than the 99th quantile of the distribution) within a 6-day temporal window of a specified conditioning site experiencing an event.

The spatial dependence models are then used to generate a 10,000-year synthetic catalogue of events. To do this, the number of events expected to occur across the UK per year was estimated from the observational record. The 99th quantile of the distribution (hereafter Q99) was used to define an extreme event at any given site, while the temporal and spatial windows

discussed above were used to group these flows into independent events. An empirical distribution was then fitted to the annual event counts.

For each year of simulation, the number of events to be generated was sampled from this distribution. This resulted in ~343,000 events, ~170,000 of which have a >1 in 5-year magnitude event in at least one catchment (the minimum magnitude for which the underlying hazard layers are calculated). Each member of the event catalogue consists of realisations of flow return periods at a set of gauge points which then need to be converted into surfaces of flood extent and depth (the flood footprint) in order to perform a loss calculation. To do this for each event, we first define catchment areas around each gauge which we assume experience the same extreme return period flow. We then determine the flood extent and depth corresponding to this return period within that zone. Assignment of gauged flows to catchment areas is performed by first discretizing the UK into independent units defined by the HydroBASINS data set (Lehner and Grill, 2013). A hybrid layer based on the level 10 basins, subdividing to level 12 basins where higher population densities are found is used. This results in ~2400 catchments across the UK which we assume experience the same event return period during a flood. Ungauged fluvial catchments have their values inferred from the most appropriate neighbouring gauge site value during a given event, defined using a distance measure based on the relative differences in upstream accumulation and spatial distance between each ungauged catchment unit and each gauge, as well as considering river network connectivity and the HydroBASINS unit ID. Ungauged pluvial and coastal catchments have their values inferred from the nearest pluvial and coastal gauge site respectively. Flood extent and depths associated with the event return period assigned to each hydrological unit are then extracted from the pre-computed library of flood hazard layers for each catchment, during each synthetic event, resulting in a complete surface of expected hazard intensity for the given footprint.

Stochastic model results were validated in three ways (see Figure S4). First, we compared observed and modelled values for the 1 in 5-year return period event at each gauge site in Figure S3 in terms of proportional absolute errors (Figure S4a). Next, we compared the observed and modelled mean event footprint size for each gauge when it is the largest (i.e., when it is the conditioning site) during a particular event (Figure S4b). Footprint size is defined as the total number of other gauge sites in the network where the river flow/rainfall/coastal water level is above the Q99 value. Finally, Figure S4c shows the cumulative distribution of the distance between a conditioning site and all other gauges which are greater than Q99 during an event. This is calculated on an event-by-event basis for both the model (in blue) and observations (in red), with the distances binned into 50km bins.
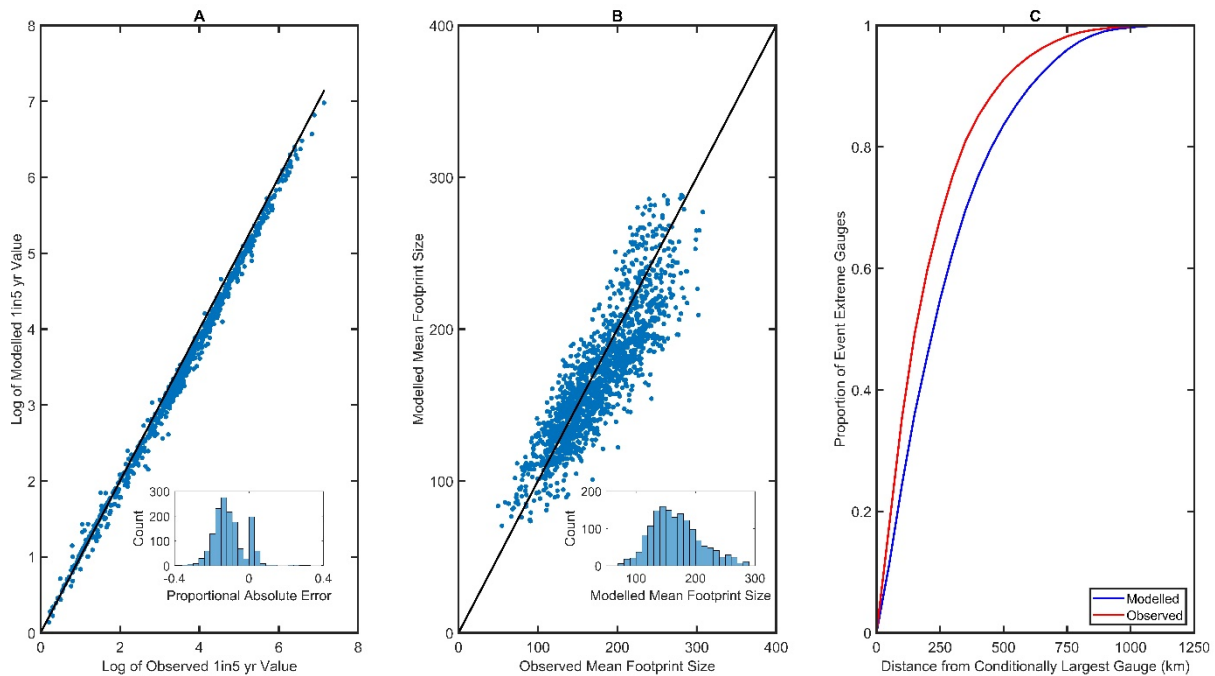
Figure S4: Validation of the stochastic model for generating synthetic flood event footprints. Panel (a) shows observed and modelled values for the 1 in 5-year return period event at each gauge site in Figure S3 in terms of proportional absolute errors. A log scale is used due to the very wide range of values given we display results for river flow, rainfall and coastal water level. Panel (b) shows observed and modelled mean event footprint size for each gauge when it is the largest during a particular event (i.e., when it is the conditionally largest gauge). Footprint size is defined simply as the number of other gauge sites in the network where the hazard intensity is greater than the 99th percentile (Q99) during each event. Panel (c) shows the observed and modelled cumulative distribution function of the distances between the largest gauge during an event and all other gauge sites experiencing hazard intensity greater than Q99. Values are calculated and accumulated on an event-by-event basis and then binned into 50km bins.

Figure S4 shows that stochastic model can reproduce both the magnitude of UK flood events (panel a) and their areal extent (panels b and c). Panel (c) also shows that the model correctly captures the observation that extreme gauge sites during an event tend to be proximate rather than distal: 80% of gauge sites experiencing > 1 in 5-year return period hazard intensity during UK flood events are within ~350km of each other in the observations and ~450km in the model. This is because, even in a small country such as the UK, most flood events are regional rather than national.

Lastly, to give an idea of what the model output looks like the footprints of two example stochastically generated synthetic events are shown in Figure S5. Event (a) represents a major inland flood affecting the lower River Severn valley, the UK Midlands and North East and bears a striking resemblance to the widespread flooding that occurred in June 2007 (Coulthard and Frostick, 2010; Marsh and Hannaford, 2007; Pitt, 2008). Event (b) represents a coastal flood that is typical of those created by Atlantic depressions and extra-tropical cyclones. Further events (not shown here) show similarly plausible patterns.
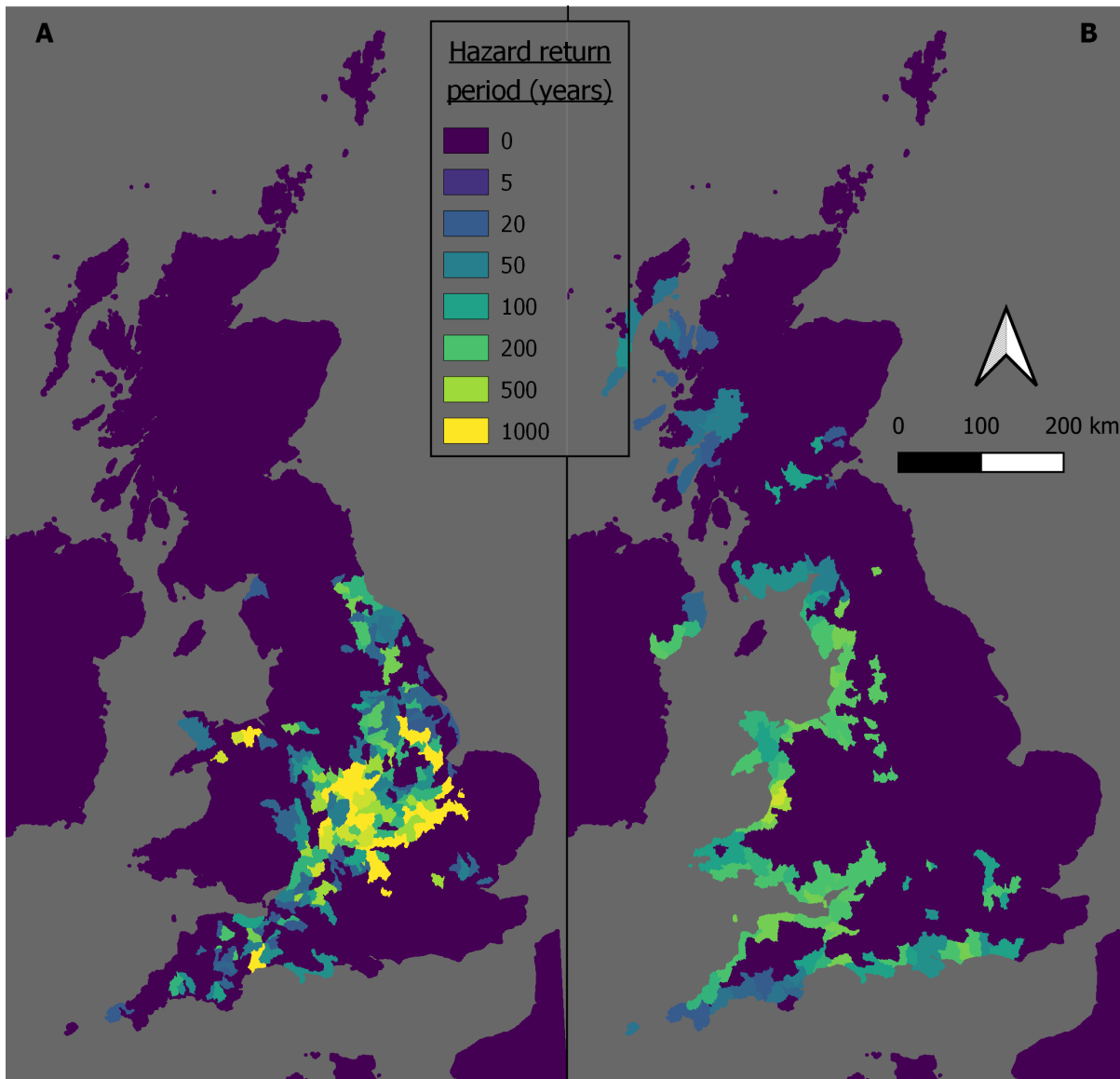
Figure S5: Intensity footprints for two synthetic flood events generated by the conditional exceedance model. Panel (a) represents a major inland event with a spatial pattern similar to Summer 2007, whilst panel (b) represents a coastal event of the kind generated in the UK by Atlantic extra-tropical cyclones. Both events form part of the stress tests used by the Bank of England's Prudential Regulation Authority to assess the resilience of the UK insurance sector to climate shocks (see https://www.bankofengland.co.uk/-/media/boe/files/prudential-regulation/letter/2022/may/ist-2022-general-insurance-scenario-specification-guidelines-instruction.pdf).

485

3.3 Financial loss calculation

490   Given maps of hazard intensity (water depth) for each event in the stochastic catalogue we calculate a financial loss by applying vulnerability functions for different property classes based on the decades of research and data collection carried out at the Middlesex University Flood Hazard Research Centre, and published in the Centre's Multi-Coloured Manual (hereafter, MCM; Penning-Rowsell et al., 2013). The MCM consists of unique vulnerability functions which discriminate between different types of flooding (pluvial, fluvial, coastal) as well as different types of insurance cover, and include predictions of Additional

495   Living Expenses (ALE) arising from the flooding of residential properties and business interruption losses. The residential damage functions account for structure and contents losses dependent on occupancy, construction and building type, ground floor height, building age, number of stories, and occupied floors. Similarly, the wide variety of non-residential curves – ranging from retail, offices and warehouses to schools, hospitals, and sports centres – are split by ground floor height, number of stories, and occupied floors. To implement this complexity, the loss computations are performed using the Oasis Loss

500   Modelling Framework (OasisLMF), an open-source catastrophe risk modelling software (see https://oasislmf.org/).

The MCM depth–damage relationships are 'synthetic', meaning they are a synthesis of multiple data sources. Post-flood damage assessments are often inaccurate, meaning reliance solely on empirical data can lead to poor loss functions. MCM curves are therefore based on an amalgamation of survey data, "what if" scenarios, insurance claims, reports from loss adjusters and quantity surveyors that is drawn together using expert judgement by specialists. More information on the philosophy

505   underpinning the development of synthetic functions can be found in Penning-Rowsell & Chatterton (1977).

MCM data were primarily developed for economic appraisals carried out by the UK government, meaning transfer payments within the economy (such as VAT) are not considered a loss and the depreciated value of items is used rather than replacement value. To translate these values to financial loss, relevant for the insurance industry, corrections to the economic functions are applied in line with the guidance and data provided in the MCM.

510   MCM curves are presented as absolute damages for a given flood depth (in 2020 GBP), while OasisLMF requires relative vulnerability functions (as a proportion of total value). Both approaches are defensible, and the academic literature does not favour one approach over another. Wing et al. (2020) illustrated that relative flood damages are not constant across all building values yet are not completely invariant either. To translate the absolute MCM curves to relative ones for application in OasisLMF we divide them by relevant measures of replacement cost. For different residential structures we use estimates of

515   construction   cost   based   on   guidelines   set   out   by   the   Royal   Institution   of   Chartered   Surveyors (https://www.rics.org/uk/upholding-professional-standards/sector-standards/), and for contents losses we obtained typical contents values for different types of residential building from a leading UK insurer.

Finally, building data are taken from the Verisk UKBuildings data set available for academic use through Digimap (https://digimap.edina.ac.uk/verisk) which gives information on property type, use status (residential, commercial or derelict),

520   age, floor area, number of storeys and even details of the substructure (e.g. presence of a basement) for each building in the

UK. This provides sufficient information to select the appropriate MCM vulnerability curve for each building and compute the loss for a given hazard intensity.

References

Allen, G. H., David, C. H., Andreadis, K. M., Hossain, F., and Famiglietti, J. S.: Global Estimates of River Flow Wave
525 Travel Times and Implications for Low-Latency Satellite Data, Geophysical Research Letters, 0, https://doi.org/10.1029/2018GL077914, 2018.

Almeida, G. A. M. and Bates, P.: Applicability of the local inertial approximation of the shallow water equations to flood modeling, Water Resources Research, 49, 4833–4844, https://doi.org/10.1002/wrcr.20366, 2013.

Almeida, G. A. M., Bates, P., Freer, J. E., and Souvignet, M.: Improving the stability of a simple formulation of the shallow
530 water equations for 2-D flood modeling, Water Resources Research, 48, https://doi.org/10.1029/2011WR011570, 2012.

Andreadis, K. M., Schumann, G. J.-P., and Pavelsky, T.: A simple global river bankfull width and depth database, Water Resources Research, 49, 7164–7168, https://doi.org/10.1002/wrcr.20440, 2013.

Bates, P. D., Horritt, M. S., and Fewtrell, T. J.: A simple inertial formulation of the shallow water equations for efficient two-dimensional flood inundation modelling, Journal of Hydrology, 387, 33–45,
535 https://doi.org/10.1016/j.jhydrol.2010.03.027, 2010.

Bates, P. D., Quinn, N., Sampson, C., Smith, A., Wing, O., Sosa, J., Savage, J., Olcese, G., Neal, J., Schumann, G., Giustarini, L., Coxon, G., Porter, J. R., Amodeo, M. F., Chu, Z., Lewis-Gruss, S., Freeman, N. B., Houser, T., Delgado, M., Hamidi, A., Bolliger, I., McCusker, K., Emanuel, K., Ferreira, C. M., Khalid, A., Haigh, I. D., Couasnon, A., Kopp, R., Hsiang, S., and Krajewski, W. F.: Combined modelling of US fluvial, pluvial and coastal flood hazard under current and
540 future climates, Water Resources Research, 57, e2020WR028673, https://doi.org/10.1029/2020WR028673, 2021.

Coulthard, T. j. and Frostick, L. e.: The Hull floods of 2007: implications for the governance and management of urban drainage systems, Journal of Flood Risk Management, 3, 223–231, https://doi.org/10.1111/j.1753-318X.2010.01072.x, 2010.

Environment Agency: Flooding in England: national assessment of flood risk, Environment Agency, Bristol, 2009.

Environment Agency: Coastal flood boundary conditions for the UK: 2018 update, Bristol, UK, 2019.

545 Hall, J. W., Dawson, R. J., Sayers, P. B., Rosu, C., Chatterton, J. B., and Deakin, R.: A methodology for national-scale flood risk assessment, Proceedings of the Institution of Civil Engineers - Water and Maritime Engineering, 156, 235–247, https://doi.org/10.1680/wame.2003.156.3.235, 2003.

Harman, C., Stewardson, M., and DeRose, R.: Variability and uncertainty in reach bankfull hydraulic geometry, Journal of Hydrology, 351, 13–25, https://doi.org/10.1016/j.jhydrol.2007.11.015, 2008.

550 Heffernan, J. E. and Tawn, J. A.: A conditional approach for multivariate extreme values (with discussion), Journal of the Royal Statistical Society: Series B (Statistical Methodology), 66, 497–546, https://doi.org/10.1111/j.1467-9868.2004.02050.x, 2004.

Hosking, J. R. M.: L-Moments: Analysis and Estimation of Distributions Using Linear Combinations of Order Statistics, Journal of the Royal Statistical Society. Series B (Methodological), 52, 105–124, 1990.

555 Kay, A. L., Rudd, A. C., Fry, M., Nash, G., and Allen, S.: Climate change impacts on peak river flows: Combining national-scale hydrological modelling and probabilistic projections, Climate Risk Management, 31, 100263, https://doi.org/10.1016/j.crm.2020.100263, 2021.

Keef, C., Svensson, C., and Tawn, J. A.: Spatial dependence in extreme river flows and precipitation for Great Britain, Journal of Hydrology, 378, 240–252, https://doi.org/10.1016/j.jhydrol.2009.09.026, 2009.

560 Keef, C., Tawn, J. A., and Lamb, R.: Estimating the probability of widespread flood events, Environmetrics, 24, 13–21, https://doi.org/10.1002/env.2190, 2012.

Keller, V. D. J., Tanguy, M., Prosdocimi, I., Terry, J. A., Hitt, O., Cole, S. J., Fry, M., Morris, D. G., and Dixon, H.: CEH-GEAR: 1 km resolution daily and monthly areal rainfall estimates for the UK for hydrological and other applications, Earth System Science Data, 7, 143–155, https://doi.org/10.5194/essd-7-143-2015, 2015.

565 Kopp, R. E., Horton, R. M., Little, C. M., Mitrovica, J. X., Oppenheimer, M., Rasmussen, D. J., Strauss, B. H., and Tebaldi, C.: Probabilistic 21st and 22nd century sea-level projections at a global network of tide-gauge sites, Earth's Future, 2, 383–406, https://doi.org/10.1002/2014EF000239, 2014.

Kovats, S. and Brisley, R.: Health, communities and the built environment, in: The Third UK Climate Change Risk Assessment Technical Report, edited by: Betts, R. A., Haward, A. B., and Pearson, K. V., The Committee for Climate
570 Change, London, UK, 2021.

Lehner, B. and Grill, G.: Global river hydrography and network routing: baseline data and new approaches to study the world's large river systems, Hydrological Processes, 27, 2171–2186, https://doi.org/10.1002/hyp.9740, 2013.

Leopold, L. B. and Maddock, T.: The hydraulic geometry of stream channels and some physiographic implications, US Government Printing Office, 1953.

575 Lewis, E., Quinn, N., Blenkinsop, S., Fowler, H. J., Freer, J., Tanguy, M., Hitt, O., Coxon, G., Bates, P., and Woods, R.: A rule based quality control method for hourly rainfall data and a 1 km resolution gridded hourly rainfall dataset for Great Britain: CEH-GEAR1hr, Journal of Hydrology, 564, 930–943, https://doi.org/10.1016/j.jhydrol.2018.07.034, 2018.

L'homme, J., Sayers, P., Gouldy, B., Samuels, P., Wills, M., and Mulet-Marti, J.: Recent development and application of a rapid flood spreading method, in: Flood Risk Management: Research and Practice, https://doi.org/10.1201/9780203883020,
580 2009.

Marsh, T. and Hannaford, J.: The summer 2007 floods in England & Wales – a hydrological appraisal, Centre for Ecology and Hydrology, 2007.

Muis, S., Verlaan, M., Winsemius, H. C., Aerts, J. C. J. H., and Ward, P. J.: A global reanalysis of storm surges and extreme sea levels, Nature Communications, 7, 11969, https://doi.org/10.1038/ncomms11969, 2016.

585 Neal, J., Schumann, G., and Bates, P.: A subgrid channel model for simulating river hydraulics and floodplain inundation over large and data sparse areas, Water Resources Research, 48, https://doi.org/10.1029/2012WR012514, 2012.

Neal, J., Dunne, T., Sampson, C., Smith, A., and Bates, P.: Optimisation of the two-dimensional hydraulic model LISFOOD-FP for CPU architecture, Environmental Modelling and Software., 107, 148–157, 2018.

Neal, J., Hawker, L., Savage, J., Durand, M., Bates, P., and Sampson, C.: Estimating River Channel Bathymetry in Large
590   Scale Flood Inundation Models, Water Resources Research, 57, e2020WR028301, https://doi.org/10.1029/2020WR028301,
2021.

Neal, J. C., Fewtrell, T. J., Bates, P. D., and Wright, N. G.: A comparison of three parallelisation methods for 2D flood
inundation models, Environmental Modelling & Software, 25, 398–411, https://doi.org/10.1016/j.envsoft.2009.11.007, 2010.

Penning-Rowsell, E., Priest, S., Parker, D., Morris, J., Tunstall, S., Viavattene, C., Chatterton, J., and Owen, D.: Flood and
595   Coastal Erosion Risk Management: A Manual for Economic Appraisal, Routledge, London, 448 pp.,
https://doi.org/10.4324/9780203066393, 2013.

Penning-Rowsell, E. C.: Comparing the scale of modelled and recorded current flood risk: Results from England, Journal of
Flood Risk Management, 14, e12685, https://doi.org/10.1111/jfr3.12685, 2021.

Penning-Rowsell, E. C. and Chatterton, J. B.: The benefits of flood alleviation: a manual of assessment techniques, Saxon
600   House, Farnborough, Eng., 1977.

Pitt, M.: Learning lessons from the 2007 floods, The National Archives, 2008.

Quinn, N., Bates, P. D., Neal, J., Smith, A., Wing, O., Sampson, C., Smith, J., and Heffernan, J.: The Spatial Dependence of
Flood Hazard and Risk in the United States, Water Resources Research, 55, 1890–1911,
https://doi.org/10.1029/2018WR024205, 2019.

605   Robson, A. J. and Reed, D. W.: Statistical procedures for flood frequency estimation, Centre for Ecology & Hydrology,
Wallingford, UK, 1999.

Sampson, C. C., Smith, A. M., Bates, P. D., Neal, J. C., Alfieri, L., and Freer, J. E.: A high-resolution global flood hazard
model, Water Resources Research, 51, 7358–7381, https://doi.org/10.1002/2015WR016954, 2015.

Sayers, P.: Projections of future flood risk in the UK, Climate Change Committee, London, UK, 2017.

610   Sayers, P. B., Horritt, M. S., Carr, S., Kay, A., Mauz, L., Lamb, R., and Penning-Rowsell, E.: Third UK Climate Change
Risk Assessment (CCRA3) future flood risk: main report, The Committee for Climate Change, 2020.

Schwanghart, W. and Scherler, D.: Short Communication: TopoToolbox 2 – MATLAB-based software for topographic
analysis and modeling in Earth surface sciences, Earth Surface Dynamics, 2, 1–7, https://doi.org/10.5194/esurf-2-1-2014,
2014.

615   Seibert, J. and Vis, M. J. P.: Teaching hydrological modeling with a user-friendly catchment-runoff-model software package,
Hydrology and Earth System Sciences, 16, 3315–3325, https://doi.org/10.5194/hess-16-3315-2012, 2012.

Shaw, J., Kesserwani, G., Neal, J., Bates, P., and Sharifian, M. K.: LISFLOOD-FP 8.0: the new discontinuous Galerkin
shallow-water solver for multi-core CPUs and GPUs, Geoscientific Model Development, 14, 3577–3602,
https://doi.org/10.5194/gmd-14-3577-2021, 2021.

620   Wing, O. E. J., Bates, P. D., Sampson, C. C., Smith, A. M., Johnson, K. A., and Erickson, T. A.: Validation of a 30 m
resolution flood hazard model of the conterminous United States, Water Resources Research, 53, 7968–7986,
https://doi.org/10.1002/2017WR020917, 2017.

Wing, O. E. J., Bates, P. D., Neal, J. C., Sampson, C. C., Smith, A. M., Quinn, N., Shustikova, I., Domeneghetti, A., Gilles, D. W., Goska, R., and Krajewski, W. F.: A New Automated Method for Improved Flood Defense Representation in Large-Scale Hydraulic Models, Water Resources Research, 55, 11007–11034, https://doi.org/10.1029/2019WR025957, 2019.

625